ELSEVIER

Journal of Power Sources 71 (1998) 361–369

JOURNAL OF POWER SOURCES

The development of intermediate-temperature solid oxide fuel cells for the next millennium

K. Choy*, W. Bai, S. Charojrochkul, B.C.H. Steele

Department of Materials, Imperial College of Science, Technology and Medicine, London SW7 2BP, UK

Abstract

Solid oxide fuel cells (SOFCs) have been rapidly developed for efficient power generation applications. One of the major activities at Imperial College concerns the development of intermediate-temperature SOFCs, and the exploitation of cost-effective fabrication processes to address the crucial technical problems which have hindered the commercialisation of SOFCs. These involve the strategic investigation on the development of planar supported thin film electrolyte PEN (positive electrode/electrolyte/negative electrode) structure [La(Sr)MnO_3/Zr(Y)O_{2-x}/Ni-ZrO_2], and SOFCs based on $La_{0.9}Sr_{0.1}Ga_{0.8}Mg_{0.2}O_{3-x}$ (LSGM) electrolytes for intermediate temperature operation (700–800°C), and to exploit the electrostatic assisted vapour deposition (EAVD) and the flame assisted vapour deposition (FAVD) as novel, simple and cost-effective methods to manufacture SOFC components and multilayer PEN structure on large area substrates in an open atmosphere, in one production step. In addition, efforts have been directed towards developing cathode/electrolyte systems to improve the conductivities in planar SOFCs. Systems such as $La_{0.82}Sr_{0.18}MnO_3/(Y_2O_3)_{0.15}(CeO_2)_{0.85}$/YSZ, $La_{0.8}Sr_{0.2}CoO_3/(Y_2O_3)_{0.15}(CeO_2)_{0.85}$/YSZ, and $La_{0.8}Sr_{0.2}CoO_3/Ce_{0.8}Gd_{0.2}O_{1.9}$/YSZ have been investigated and compared with $La_{0.82}Sr_{0.18}MnO_3$/YSZ where YSZ is 8 mol% Y_2O_3 in ZrO_2. The process, structure and properties of the cell components and cathodes have been examined using SEM, XRD and AC-impedance spectroscopy. The results from these new systems indicate a superior performance in overall conductivity to the conventional $La_{0.82}Sr_{0.18}MnO_3$/YSZ system. © 1998 Elsevier Science S.A.

Keywords: Solid oxide fuel cells; Electrostatic assisted vapour deposition; Flame assisted vapour deposition; PEN structure

1. Introduction

Exploitation of solid oxide fuel cells (SOFCs) for efficient power generation has still failed to reach commercial viability due to the long-term degradation problems associated with high-temperature SOFCs and relatively expensive large scale manufacturing processes. The development of intermediate-temperature SOFCs and the exploitation of two cost-effective fabrication processes to address these technical problems have been explored at Imperial College. In the development of intermediate-temperature SOFCs, we focus on the use of thin electrolyte film based on YSZ and LSGM. For the fabrication process, we explore the technical viability of EAVD and FAVD methods for the manufacture of SOFC components.

A variety of vapour processing techniques have been examined to fabricate the films of SOFC, such as chemical vapour deposition [1], physical vapour deposition [2], electrochemical vapour deposition (EVD) [3,4]. These vapour processing methods are generally very expensive because they involved the use of sophisticated reactors and/or vacuum systems. Therefore, these methods are not viable for the commercial large-scale production. Many groups are trying to adapt conventional ceramic processing methods such as tape casting [5], screen printing [6], slurry coating [7] and colloidal method [8,9] for the preparation of PEN structures. Whilst these conventional methods are appropriate for small area configuration, the large shrinkage associated with the removal of polymeric binders and plasticisers in subsequent sintering steps reduces the quality of large area PEN assemblies. Moreover, it is often difficult to retain adequate porosity within the supporting electrode structures during the co-firing stage for densification of the thick film electrolyte. Among these techniques, EVD seems to be the only successful method in preparing dense YSZ film onto a porous substrate [3]. However, it is a very expensive processing technique as mentioned earlier, and requires a high deposition temperature and releases toxic by-products. This has prompted us to develop and explore a cost-effective deposition method called electrostatic

* Corresponding author.

0378-7753/98/$19.00
PII S0378-7753(97)02728-6

assisted vapour deposition (EAVD) [10] to manufacture SOFC components. The EAVD process involves spraying atomised precursor droplets across an electric field where the droplets undergo combustion and/or chemical reaction in the vapour phase near the vicinity of the heated substrate. The result is a stable solid film with excellent adhesion onto a substrate in a single production process. This method has been developed to deposit SOFC components such as dense $Zr(Y)O_{2-x}$ and $La_{0.9}Sr_{0.1}Ga_{0.8}Mg_{0.2}O_{3-x}$ (LSGM) electrolytes, porous $La(Sr)MnO_3$ cathode and porous NiO–YSZ anode. In comparison to other vapour deposition techniques, this method has a high deposition rate (1–5 μm/min), and allows easy control of the stoichiometry and microstructure of the deposits. In addition, it offers a potentially simplified processing route for SOFCs, and makes the process very attractive and economical for potential large-scale commercial fabrication of SOFC. Dense or porous films can be deposited simply by varying the concentration and flow rate of the precursor solution and deposition temperature. Multilayer PEN structures of different materials can be deposited in one consecutive process simply by switching precursor solutions and carefully controlling processing conditions.

In addition, a simple and cost-effective method called flame assisted vapour deposition (FAVD) has also been developed for the manufacturing of electrodes [11]. This method requires simple apparatus and the deposition can be performed in an open atmosphere in which an atomised solution is sprayed across a flame source where the decomposition and combustion reactions occurred, resulting in a stable film deposited on a heated substrate [12]. This FAVD method has been explored for the manufacturing of cathode/electrolyte system which improved the interfacial conductivity. Multilayer films of LSM/YDC/YSZ, LSC/YDC/YSZ, and LSC/CGO/YSZ have been investigated and compared with LSM/YSZ, where YDC is yttria-doped ceria. LSC is more reactive with YSZ than LSM and forms an intermediate phase; however, LSC has a higher electronic conductivity than LSM and superior electrocatalytic activity to LSM. The intermediate reactions could be minimised by depositing a thin layer of doped ceria electrolyte, which also helps to lower the cell resistance [20]. There is no reported apparent interfacial reaction between the doped ceria materials and LSC. In addition, the coefficients of thermal expansion (CTE) of CGO and YDC are in between YSZ and LSC; therefore, the problem of thermal expansion coefficient mismatch is reduced.

2. Experimental

2.1. EAVD process

2.1.1. Fabrication of planar supported thin film electrolyte PEN structure

The EAVD method involves the preparation of stable sol precursors based on alkoxides and/or nitrates with the required stoichiometry for the deposition of the $La(Sr)MnO_3$, 9 mol% YSZ, and NiO–YSZ. The sol precursor was subsequently atomised to form aerosol. The aerosol was sprayed across an electric field within a vertical tubular reactor at atmospheric pressure. The description of the deposition process of dense and porous films has been outlined in Ref. [10].

The fabrication of multilayer PEN structure ($La(Sr)MnO_3$/YSZ/Ni–YSZ) has been achieved in one production process by switching the precursor solutions for the deposition of anode, electrolyte and cathode. The supported substrate is porous LSM prepared by a conventional ceramic powder processing route. A commercial LSM powder (from Merck, Germany) was pressed into pellets of diameter 15 mm and thickness of around 0.7 mm. The pellets were sintered at 1300°C for 2 h in air. The first layer deposited onto LSM substrate was LSM with reduced porosity as compared to the substrate. This was then followed by a dense layer of YSZ film, and a layer of NiO–YSZ anode at the outermost of the PEN cell. The crystallisation behaviour of the deposited porous/dense/porous films was studied using X-ray diffraction (XRD). The microstructure of SOFC components was investigated using scanning electron microscopy (SEM).

2.1.2. Deposition of $La_{0.9}Sr_{0.1}Ga_{0.8}Mg_{0.2}O_{3-x}$ electrolyte film for intermediate-temperature SOFCs

The successful deposition of LSGM film depends on the synthesis of a stable LSGM sol precursor solution. The synthesis of a stable sol precursor for the deposition of LSGM follows the standard sol preparation procedures. A dense LSGM film was deposited onto a porous LSM substrate. The porous LSM substrates were prepared using the conventional ceramic powder processing route as outlined above. The detailed description of the deposition process of the dense LSGM has been described in references [13]. The crystallisation behaviour and microstructure of the final deposited LSGM films were investigated using XRD and SEM. AC-impedance spectroscopy was used to study the electrical properties of the LSGM films as a function of deposition temperature.

2.2. FAVD process

2.2.1. Fabrication of improved cathode/electrolyte systems

YSZ substrates were prepared by a conventional ceramic sintering method. An 8 mol% Tosoh (Japan) powder was pressed into pellets of diameter 10 mm and thickness of around 0.7 mm. They were sintered at 1500°C for 2 h in air. After sintering, the density of the pellet was greater than 98%.

The metal nitrate powders of La, Sr, Mn, Co, Ce, Gd, and Y were dissolved in water and ethanol to produce a precursor solution of 0.05 M. The ratios of compositions in the solution were in accordance with the final composition of $La_{0.82}Sr_{0.18}MnO_3$, $La_{0.8}Sr_{0.2}CoO_3$, $(Y_2O_3)_{0.15}(CeO_2)_{0.85}$, and

$Ce_{0.8}Gd_{0.2}O_{1.9}$. Multilayers of cathode/electrolyte systems were deposited by FAVD technique. The details of the deposition were described in Ref. [11]. A thin layer of dense YDC and CGO was deposited onto YSZ substrate, followed by the deposition of porous cathode (e.g. LSM or LSC) to form cathode/electrolyte systems LSM/YDC/YSZ, LSC/YDC/YSZ and LSC/CGO/YSZ.

SEM was used to examine the microstructure of the deposited films. The interfacial electrical resistance at the electrode/electrolyte interface was measured using the AC-impedance method at different temperatures in air.

3. Results and discussion

3.1. EAVD process

3.1.1. $La(Sr)MnO_3$/YSZ/NiO–YSZ PEN cells

3.1.1.1. Porous cathode $La(Sr)MnO_3$. Fig. 1 shows the cross-section of a porous LSM film on a dense YSZ substrate. The degree of porosity in the cathode films strongly depends on the flow rate of the precursor solution and the substrate temperature. Dense LSM film

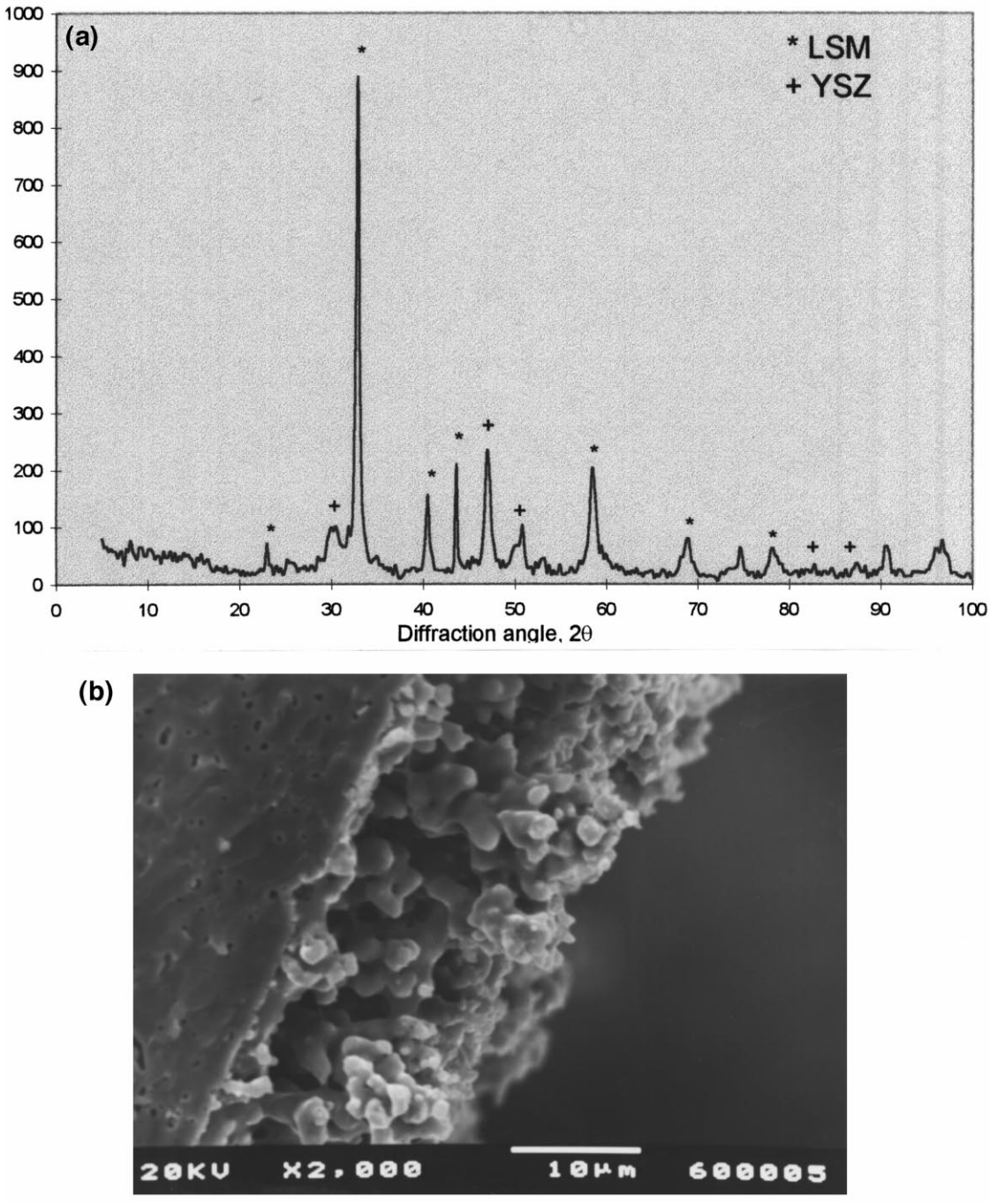

Fig. 1. (a) Typical XRD pattern of LSM films deposited using EAVD process. (b) SEM micrograph of the cross-section of LSM.

could be obtained at 400°C ≤ T ≤ 550°C and flow rate of 20 μl/min. When the substrate temperature was above 550°C and the flow rate was greater than 0.1 ml/min, porous LSM films were obtained. The deposition rate of LSM film was between 1 and 5 μm per minute depending on the concentration, flow rate of the precursor solution and substrate temperature.

The crystal phase structure of porous LSM film was mainly determined by the substrate temperature. When the porous LSM films were deposited at a lower substrate temperature (less than 500°C), the deposited LSM film was amorphous or nanocrystalline. After the sample was heat-treated to 800°C for 2 h, the crystal structure transformed to the desired perovskite phase. At a higher substrate temperature (≥650°C), it resulted in an increase in the crystallinity of the porous film as shown in the XRD trace (Fig. 1). This indicates that the deposition of crystalline perovskite LSM film could be achieved by one step at a higher substrate temperature. However, such a deposition temperature is still lower than the conventional ceramic sintering temperature (1100–1200°C) for LSM. Therefore, there is no $La_2Zr_2O_3$ presence in the deposited film as shown in Fig. 1 as compared to the literature [14,15], which generally reported the presence of $La_2Zr_2O_3$ due to the reaction between the YSZ film and LSM cathode at high temperatures during sintering process. Furthermore, it was observed that there was no Mn diffusion from the cathode LSM to the YSZ film, which has been previously reported so that the Mn diffusion could cause a Mn deficiency, hence promoting $La_2Zr_2O_7$ formation at the interface during the high-temperature sintering of the two layered samples.

3.1.1.2. Porous anode Ni–YSZ. The electrical conductivity of Ni-YSZ cermet depends on its Ni content. The percolation threshold for the conductivity of Ni–YSZ anode system is about 30 vol.% nickel. However, nickel has a higher thermal expansion coefficient than YSZ, so there are concerns about thermal expansion mismatch between the anode and electrolyte. A significant degree of mismatch in thermal expansion coefficients of the SOFC components can result in large stresses, causing cracking or delamination of anode films during fabrication and/or operation.

The thermal expansion coefficient of Ni–YSZ cermet increases linearly with the nickel content [16,17]. The cermet containing more than 30 vol.% nickel has a higher thermal expansion coefficient than the YSZ electrolyte. A large number of methods have been developed to tolerate and minimise the coefficient of thermal expansion mismatch (CTE) between the anode and electrolyte. In our experiment, the Ni–YSZ film was deposited onto YSZ substrate with a gradual increased in Ni content from 30 vol.% to 40 vol.% (at the outermost part of NiO–YSZ film) in order to minimise the CTE mismatch. Fig. 2 shows the SEM micrograph of the cross-section of NiO–YSZ film on dense YSZ substrate. It is clearly seen that the anode NiO-YSZ film is uniform with controlled pore size (about 3 μm). No cracking was observed.

3.1.1.3. Dense YSZ and multi-layer PEN structure of SOFC components. A dense YSZ film was deposited onto a porous LSM substrate at 650°C with a deposition rate of 1 μm/min. A thinner electrolyte film could be deposited onto porous LSM substrate as shown in Fig. 3, where the thickness of YSZ is about 50 μm. YSZ films 5–20 μm thick have also been deposited using the EAVD method. The cracking or spalling of the YSZ film was not observed. There was a sharp interface between the dense YSZ and the porous LSM substrate. The adhesion of YSZ film onto the substrate was good as shown in the fractured sample.

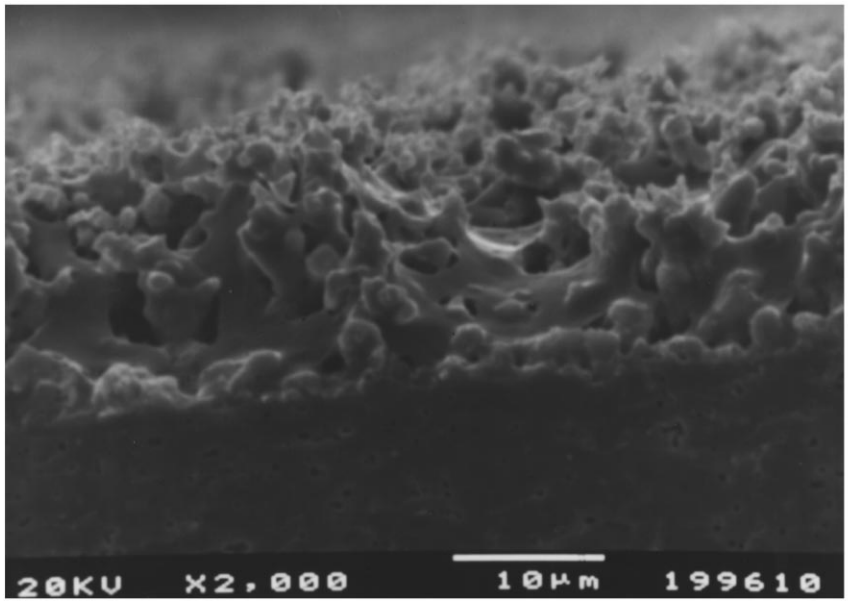

Fig. 2. An SEM micrograph of the cross-section of NiO-YSZ/YSZ structure.

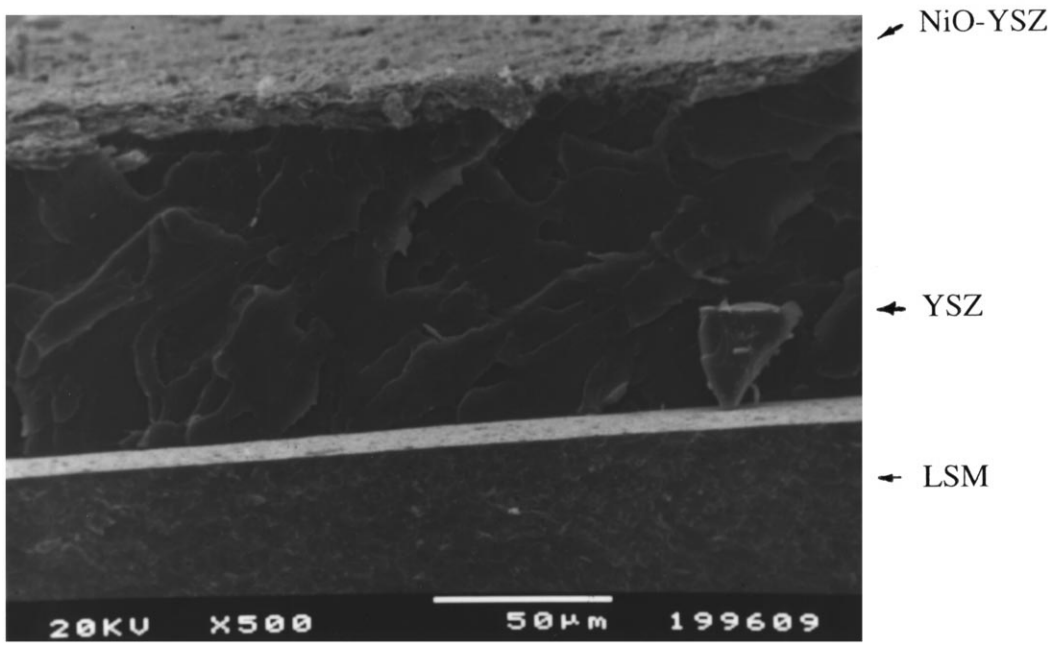

Fig. 4. An SEM micrograph of the cross-section of a multilayer PEN structure.

The prototype PEN cell structure has been successfully fabricated using the EAVD process in a single operation by controlling deposition conditions and changing the precursor solutions. The cross-section micrograph of a multilayer PEN structure is shown in Fig. 4. It shows the uniform multilayer PEN structures with clear interface. No crack or spalling was observed.

3.1.2. Dense $La_{0.9}Sr_{0.1}Ga_{0.8}Mg_{0.2}O_{3-x}$ film

The microstructure of LSGM film depends on the deposition process and sintering temperature. When the LSGM film was deposited onto a porous LSM substrate at 300–400°C, and subsequently sintered at 1000°C for 2 h, it was observed that the deposited film was dense but with some microcracks. When the LSGM film was deposited at a higher temperature, 500–600°C, followed by sintering at 1000°C for 2 h, dense and crack-free film with a small amount of pinholes was obtained (Fig. 5). A dense and crack-free film without any pinhole was obtained by repeating the deposition and sintering processes three times, as shown in Fig. 6.

The essential deposition principle of LSGM film is sol-to-

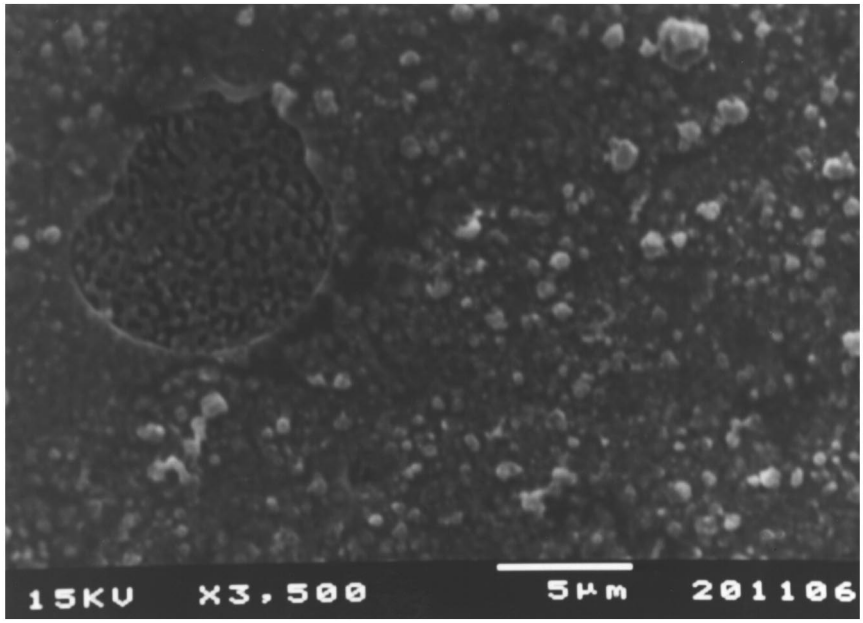

Fig. 5. An SEM micrograph of a dense LSGM film with some pinholes.

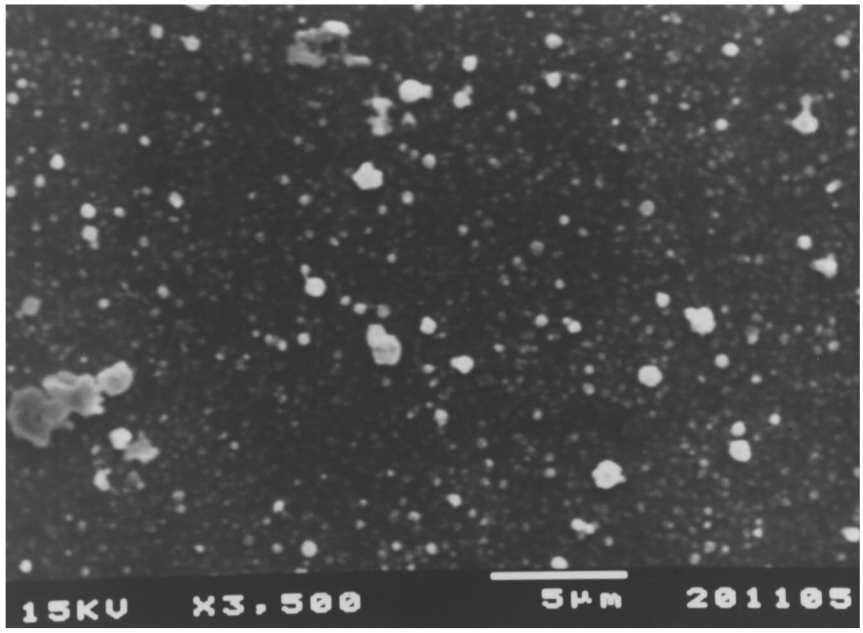

Fig. 6. An SEM micrograph of a dense and crack-free LSGM film without pinholes.

gel transition. The charged droplets of LSGM sol precursor are transformed to a gel during their transport from the discharged nozzle (positive) to substrate (negative) under the temperature gradient field. The solvent has already been evaporated when the droplets reach the substrate, and the chemical reaction occurs just on or in very close vicinity of the substrate surface to form the desired oxide phase.

Fig. 7 shows the typical XRD pattern of LSGM film. Feng and Goodenough [18] reported that the $La_{0.9}Sr_{0.1}Ga_{0.8}Mg_{0.2}O_{3-x}$ phase was cubic perovskite, but Ishihara et al. [19] have reported an orthorhombic structure for this material. In our study, the crystal structure of the $La_{0.9}Sr_{0.1}Ga_{0.8}Mg_{0.2}O_{3-x}$ film was a cubic lattice although diffraction peaks assigned to secondary phases such as La_4SrO_7 were recognised. As the ionic radius of Mg is larger than that of Ga, the presence of Mg dopant enhances the geometrical symmetry of perovskite type structure resulting

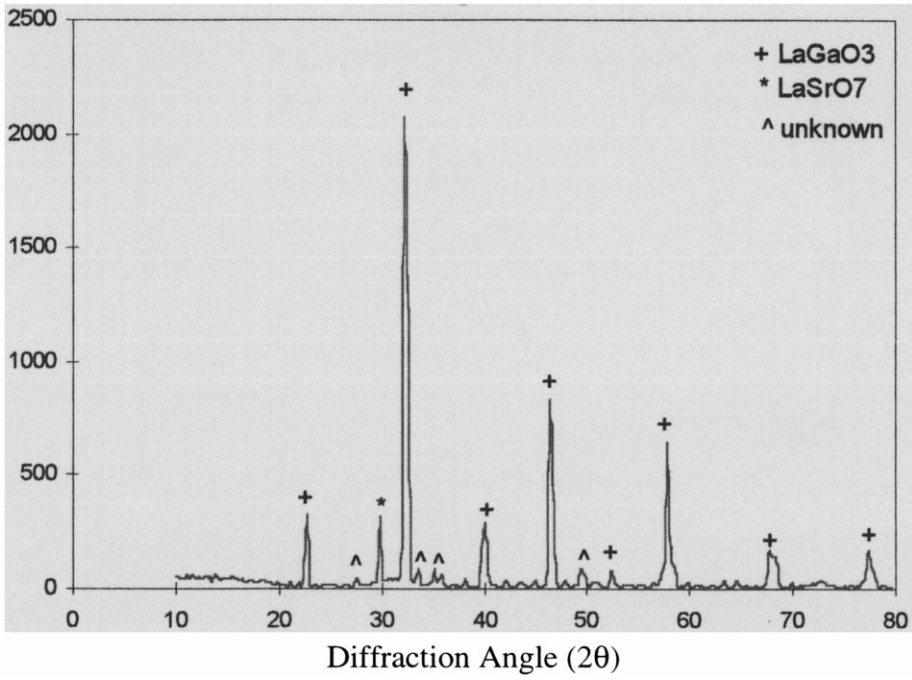

Fig. 7. A typical X-ray diffraction pattern of an LSGM film.

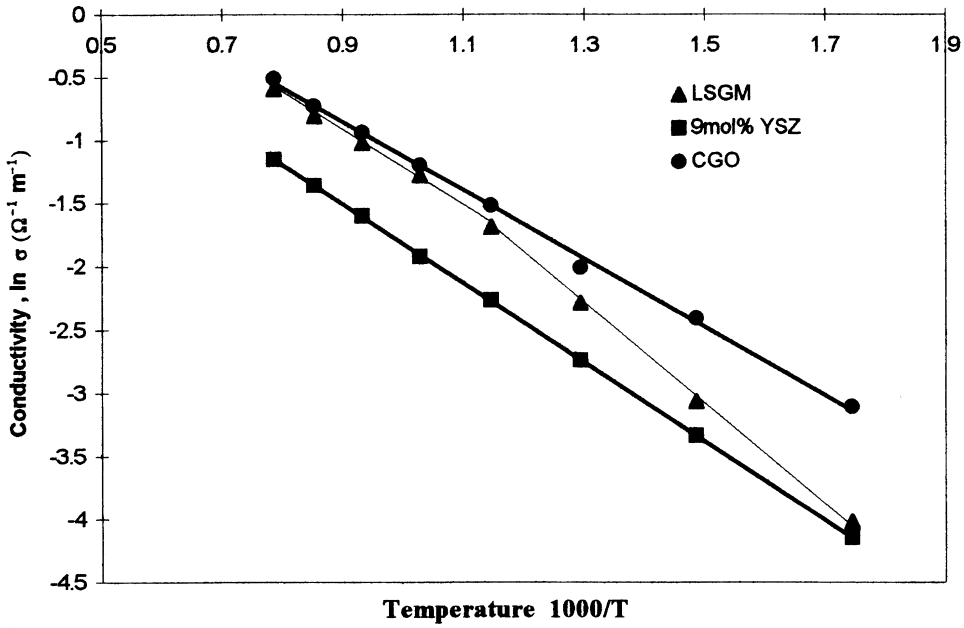

Fig. 8. Arrhenius plots of LSGM bulk conductivity versus temperature.

in a decrease in the secondary phase. On the other hand, the ionic radius of Mg is smaller than that of La. It is expected that the Mg dopant dissolved substitutionally into the lattice of B site in $LaGaO_3$. The XRD pattern of $La_{0.9}Sr_{0.1}Ga_{0.8}xMg_{0.2}O_{3-x}$ film in Fig. 7 exhibited no diffraction peaks from the compound containing Mg dopants. This implies that the substitutional solid solution has occurred and the perovskite phase of $LaGaO_3$ was obtained in this study.

Fig. 8 shows the Arrhenius plots of the bulk conductivity of LSGM as a function of temperature. The straight lines drawn are linear least-square fits to the ionic conductivity data temperature (300–600°C and 600–900°C). Apparently, the conductivity of LSGM in the temperature range 300–600°C increases faster than that in the temperature range 600–900°C as the temperature increases. At a higher temperature range 600–900°C, the activation energy of LSGM was approximately equal to that of $Ce_{0.8}Gd_{0.2}O_{2-x}$ (CGO). This implies that the ionic conductivity values of CGO are comparable with LSGM in the medium temperature range 600–800°C. Thus, we can summarise that the

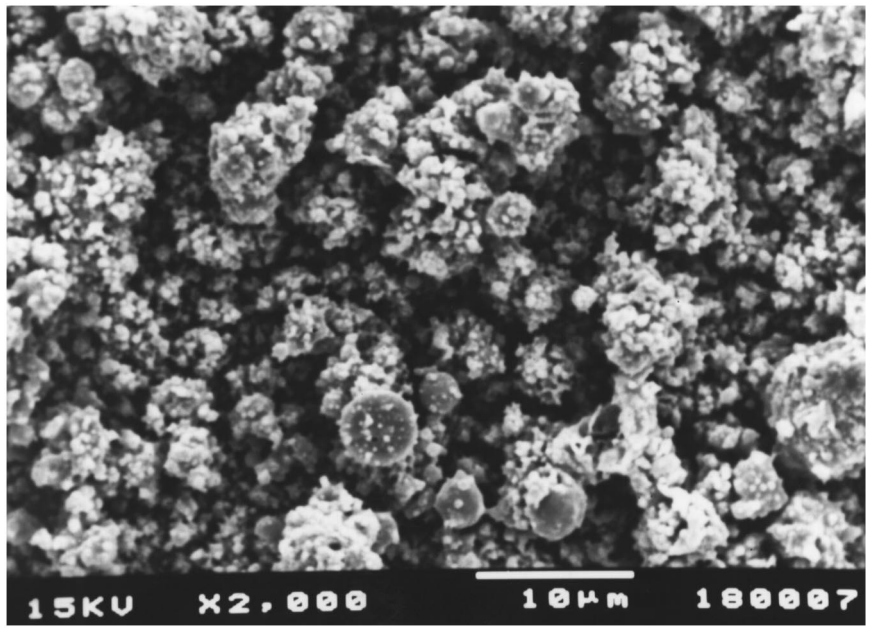

Fig. 9. An SEM micrograph of the surface morphology of an LSC film.

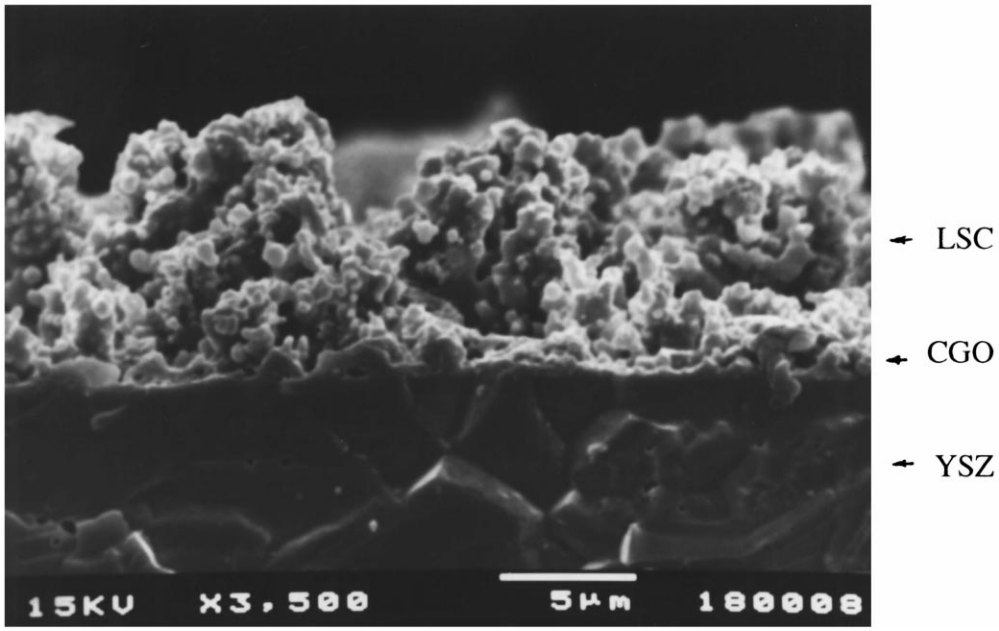

Fig. 10. An SEM micrograph of the cross-section of LSC/CGO films on YSZ substrate.

perovskite oxide film of $La_{0.9}Sr_{0.1}Ga_{0.8}Mg_{0.2}O_{3-x}$ is suitable for SOFC application in a medium temperature range (600–800°C).

3.2. FAVD process

3.2.1. The development of improved cathode/electrolyte systems

Thin layers of dense CGO and YDC were deposited onto YSZ substrate, followed by a thick porous layer of LSM or LSC. The thickness of CGO and YDC layers was around 1 μm while the cathode thickness was between 5 and 10 μm. These films adhere well to the substrate.

Figs. 9 and 10 show the surface morphology of the outer layer, LSC and cross-section of LSC/CGO/YSZ and of LSC/CGO/YSZ respectively. The particle size of the as deposited porous LSC film is around 0.5–1 μm and the total thickness of the films is about 9 μm. The agglomeration of particles occurred during sintering and increased the particle size to 2–5 μm. The porosity of the porous layer is approximately 40%.

The electrode/electrolyte interfacial resistances were measured in the temperature range 300–800°C using AC-impedance measurement on symmetrical electrode assemblies. Table 1 shows the average interfacial resistance of each system. These values have been extrapolated from the experimental results.

Table 1

The electrode/electrolyte interfacial resistance of various systems at different temperatures

System	R(800°C) Ω·cm^2	R(900°C) Ω·cm^2
LSM/YSZ[a]	7.61 (1.6) [20]	3.43 (4) [21]
LSM/YDC/YSZ	2.49	3.47
LSC/YDC/YSZ	0.038	0.015
LSC/CGO/YSZ	0.044	0.014

[a]The resistances of $La_{0.85}Sr_{0.15}MnO_3$ prepared by tape casting are approximately 0.25 Ω·cm^2 at 945°C [22]. [20]: $La_{0.8}Sr_{0.2}MnO_3$ prepared by hot drying process. [21]: $La_{0.6}Sr_{0.4}MnO_3$ prepared by slurry method.

The presence of the YDC interlayer has improved the interfacial resistance of LSM/YSZ threefold at 800°C. The LSC/YDC/YSZ system has a lower interfacial resistance at 800°C than LSC/CGO/YSZ, whereas LSC/CGO/YSZ performs better at 900°C. These resistances are better than the $La_{0.6}Sr_{0.4}CoO_{3-\delta}$/CCO/$La_{0.6}Sr_{0.4}CoO_{3-\delta}$ system fabricated by the co-precipitation technique, ~31 Ω·cm^2 at 800°C [23], where CCO is 10 mol% CaO doped CeO_2.

4. Conclusions

We have demonstrated the technical viability of both EAVD and FAVD methods in the fabrication of SOFC components. The potential of EAVD to manufacture PEN cell of LSM/YSZ/Ni-YSZ cost-effectively has also been demonstrated. The feasibility of EAVD to deposit thin electrolytes (e.g. YSZ and LSGM) with well-controlled stoichiometry has also been confirmed. This shows that EAVD could be used effectively to manufacture and develop SOFC components for operating at intermediate temperatures. The process, structure, and electrical property of these SOFC components have also been presented.

In addition, a cost-effective FAVD method has also been developed for the manufacturing of improved cathode/electrolyte systems. The FAVD technique has been shown to be capable of depositing both dense and porous films of the cathode/electrolyte systems. The interfacial resistance can be improved with an interlayer of electrolytes, YDC and

CGO. These interlayers allow the use of LSC cathode with YSZ electrolyte instead of the conventional LSM, which has lowered the interfacial resistance two-fold.

Acknowledgements

The financial support provided by the Royal Society and EPSRC (GR/K/86954) is gratefully acknowledged. S.C. wishes to express her special gratitude to the Government of Thailand for her PhD scholarship.

References

[1] Y.B. Kim, S.G. Yoon and H.G. Kim, *J. Electrochem. Soc., 139* (1992) 2559.
[2] E.S. Thiele, L.S. Wang, T.O. Wangand and S.A. Barnett, *J. Vac. Sci. Technol., 49* (1991) 3054.
[3] U.B. Pal and S.C. Singhal, *J. Electrochem. Soc., 137* (1990) 2937.
[4] C. Tanner, J.F. Jue and A.V. Virkar, *J. Electrochem. Soc., 140* (1993) 1073.
[5] N.Q. Minh, T.R. Armstrong, J.R. Esopa, J.V. Guiheen, C.R. Home and J.J. van Ackeren, in *Proc. 3rd Int. Symp. Solid Oxide Fuel Cell*, Vol. 93–4, The Electrochemical Society, 1993, p. 801.
[6] R. Yamaguchi, K. Hashimoto, H. Sakata, H. Kajiware, K. Watanable, T. Setiguchi, K. Eguchi and H. Arai, in *Proc. 3rd Int. Symp. Solid Oxide Fuel Cell*, Vol. 93–4, The Electrochemical Society, 1993, p. 704.
[7] V.E.J. Van Dieten, P.H.M. Walterbos and J. Schoonman, *Proc. 2nd Int. Symp. Solid Oxide Fuel Cell*, The Electrochem. Soc., 1991, p. 183.
[8] J. Divisek, L.G.J. DeHaart, P. Holtappels, T. Lennartz and W. Mallener, *J. Power Sources, 49 (1–3)* (1994) 257.
[9] S. DeSouza, S.J. Visco and L.C. DeJonghe, *J. Electrochem. Soc., 144* (1997) L35.
[10] K.L. Choy, W. Bai and B.C.H. Steele, in U. Stimming, S.C. Singhal, H. Tagawa and W. Lehnert (eds.), *Proc. 5th Int. Symp. SOFCs*, Aachen, Germany, June 1997, The Electrochemical Society, Pennington, NJ, 1997, p. 1177.
[11] K.L. Choy, S. Charojrochkul and B.C.H. Steele, *Solid State Ionics, 96* (1997) 49.
[12] I. Wiedmann, K.L. Choy and B. Darby, in *British Ceram. Proc., Convention 1994*, York, UK, April, 1994, The Institute of Materials, 1994, p. 133.
[13] K.-L. Choy, W. Bai and B.C.H. Steele, *International Energy Association Workshop*, Ovronnaz, Switzerland, January, 1997.
[14] N. Kimura, H. Okamuraand J. Morishita, *Adv. Ceram., 24* (1988) 183.
[15] S. Maschio, E. Bischoff, O. Sbaizeroand S. Meriani, *Zirconia, 88* (1989) 171.
[16] M.T. Claar and B. Flandermeyer, *J. Am. Ceram. Soc., 69* (1986) 628.
[17] T. Easler, B.K. Flandermeyer, T.K. Claar, D.E. Bush, R.J. Fousek, J.J. Picciolo and R.B. Poeppel, *1986 Fuel Cell Seminar Abstracts* (Tucson, AZ, Oct, 1986), Courtesy Associates, Wasington, DC, 1986.
[18] M. Feng and J.B. Goodenough, *Eur. J. Solid State Inorg. Chem., 31* (1994) 663.
[19] T. Ishhihara, H. Matsuda and Y. Takita, *J. Am. Chem. Soc., 116* (1994) 3801.
[20] T. Tsai and S.A. Barnett, in U. Stimming, S.C. Singhal, H. Tagawa and W. Lehnert (eds.), *Proc. 5th Int. Symp. SOFCs*, Aachen, Germany, June 1997, The Electrochemical Society, Pennington, NJ, 1997, p. 274.
[21] K. Eguchi, T. Inoue, M. Ueda, J. Kaminae and H. Arai, in F. Gross, P. Zegers, S.C. Singhal and O. Yamamoto (eds.), *Proc. 2nd Int. Symp. SOFCs*, Athens, Greece, July 1991, Commission of the European Communities, Luxembourg, 1991, p. 697.
[22] F.H. van Heuveln and H.J.M. Bouwmeester, *J. Electrochem. Soc., 144 (1)* (1997) 134.
[23] K. Masuda, A. Kaimai, K. Kawamura, Y. Nigara, T. Kawada, J. Mizusaki, H. Yugami and H. Arashi, in U. Stimming, S.C. Singhal, H. Tagawa and W. Lehnert (eds.), *Proc. 5th Int. Symp. SOFCs*, Aachen, Germany, June 1997, The Electrochemical Society, Pennington, NJ, 1997, p. 473.